

CO/Ethene Copolymerization at Zirconocene Centers?

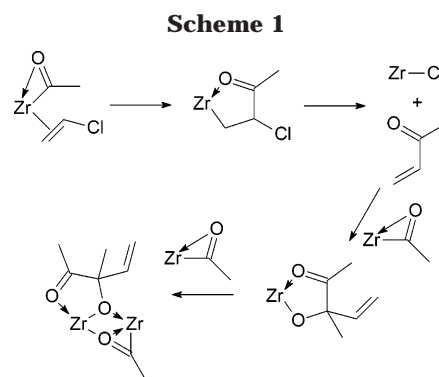
Peter H. M. Budzelaar[†]*Metal-Organic Chemistry (Dutch Polymer Institute), University of Nijmegen, Nijmegen, The Netherlands*

Received November 9, 2003

The alternating copolymerization of CO and ethene at the zirconocene centers Cp₂Zr, Me₂-SiCp₂Zr, and *rac*-Me₂SiInd₂Zr was investigated by DFT methods. CO coordinates much more strongly than ethene but has a rather high insertion barrier. Thus, propagation is slowed dramatically but the growing chains will not necessarily all incorporate CO. Secondary alkyls insert CO more efficiently than primary alkyls. After the first CO insertion, subsequent olefin and CO insertions will alternate. Olefin insertion will be very slow at high CO pressures, but at low [CO] the olefin and CO insertion barriers are comparable and are lower than that of the first CO insertion. Use of CO as a quenching and chain-counting method appears to be safe, *provided* a high pressure of CO is employed and the quenched reaction is not worked up at low temperature.

Introduction

Olefin polymerization is catalyzed by both early (Ti, Zr, V)¹ and late (Fe, Co, Ni, Pd)² transition metals. The much more recently discovered alternating copolymerization of olefins and carbon monoxide is catalyzed by a few late transition metals only (typically Pd and Ni).³ Early transition metals are capable of both olefin and CO insertion into the metal–carbon bond. Indeed, CO insertion into zirconacyclopentanes, zirconacyclopentenes, and zirconacyclopentadienes has been used in the synthesis of cyclopentanones and related compounds.⁴ However, the high oxophilicity of these metals was expected to block further insertion at some stage of the reaction. Indeed, CO is frequently used to quench polymerization reactions at early transition metals and so count the number of growing chains.^{5,6} Therefore, the observation by Busico⁷ that metallocene polymerization, when quenched with CO, produced chains containing oligo-ketone end groups came as a surprise. In the first place, this can be an unwelcome complication, since it makes the use of (possibly labeled) CO for counting chains problematic. Second, it raises a number of fundamental questions regarding the mechanism and rate-limiting steps of the copolymerization. Finally, if this copolymerization could be carried out in a reasonably efficient manner, it might enable the production of apolar polyolefin chains bearing highly polar oligo-ketone end groups, which should result in interesting



surface properties such as improved adhesion and paintability.

At present, the generality of the results reported by Busico⁷ is not clear. CO quenching is a standard tool for chain counting, but the results reported to date do not indicate that it routinely leads to oligo-ketone end groups. For example, Fukui⁶ suggested that all chains are terminated by a single CO moiety, leading to fully blocked polymerization and eventually to aldehyde end groups. Relatively little work has been done on CO insertion in well-defined cationic zirconocene alkyls. Jordan has reported CO insertion in Cp₂ZrMe⁺ and Cp^{*}₂ZrMe⁺ fragments and observed multiple (alternating) insertions of CO and *alkynes*.⁸ The X-ray structures of both Cp₂Zr(η²-COMe)(CO)⁺⁹ and Cp^{*}₂Zr(η²-COMe)(CO)⁺¹⁰ have been determined. The substituted olefin vinyl chloride was found to react with Cp₂Zr(η²-COMe)(CO)⁺ via 1,2-insertion; a cascade of reactions eventually led to a dinuclear acyl complex (Scheme 1).

No theoretical study on insertion in cationic alkyls has appeared. CO insertion in *neutral* Cp₂ZrMe₂, leading first to Cp₂Zr(Me)(η²-COMe) and then to Cp₂Zr(η²-

[†] To whom correspondence should be addressed. E-mail: budz@sci.kun.nl.

(1) *Polypropylene Handbook*; Moore, E. P., Jr., Ed.; Hanser: New York, 1996.

(2) Ittel, S. D.; Johnson, L. K. *Chem. Rev.* **2000**, *100*, 1169.

(3) Drent, E.; Budzelaar, P. H. M. *Chem. Rev.* **1996**, *96*, 663.

(4) Xi, Z.; Fan, H.-T.; Mito, S.; Takahashi, T. *J. Organomet. Chem.* **2003**, *682*, 108 and references cited therein.

(5) (a) Matsko, M. A.; Bukatov, G. D.; Mikenas, T. B.; Zakharov, V. A. *Macromol. Chem. Phys.* **2001**, *202*, 1435. (b) Bukatov, G. D.; Zakharov, V. A. *Macromol. Chem. Phys.* **2001**, *202*, 2003.

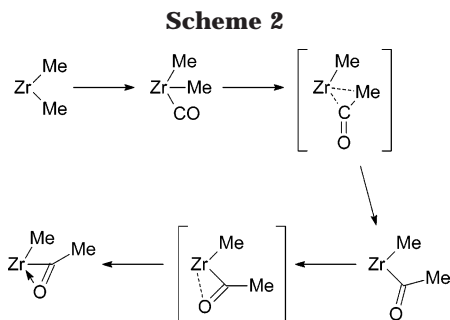
(6) Fukui, Y.; Murata, M. *Macromol. Chem. Phys.* **2001**, *202*, 1430.

(7) Busico, V.; Guardasole, M.; Margonelli, A.; Segre, A. L. *J. Am. Chem. Soc.* **2000**, *122*, 5226.

(8) Guram, A. S.; Guo, Z.; Jordan, R. F. *J. Am. Chem. Soc.* **1993**, *115*, 4902.

(9) Shen, H.; Jordan, R. F. *Organometallics* **2003**, *22*, 2080.

(10) Guo, Z.; Swenson, D. C.; Guram, A. S.; Jordan, R. F. *Organometallics* **1994**, *13*, 766.



Me₂CO), has been studied theoretically by Sgamellotti.¹¹ They found the first insertion to be a two-step process (Scheme 2). CO preferentially enters from the side; via a three-center transition state it forms an “O-out” η^1 acyl complex. This is only a shallow local minimum, which has a barrier of ca. 0.6 kcal/mol for rearrangement to the much more stable η^2 -acyl complex.

In the current paper, we use DFT calculations to clarify the possibility of multiple CO/olefin insertions in zirconocene catalysts and to elucidate mechanistic details. In addition, we will discuss the implications for the use of CO quenching as a counting method.

Methods

All calculations were carried out with the Turbomole program¹² coupled to the PQS Baker optimizer.¹³ Geometries were fully optimized as minima or transition states at the b3-lyp level¹⁴ using the Turbomole SVP basis set on all atoms (def-SVP pseudopotential basis on Zr) and a fine (“m4”) integration grid. All stationary points were characterized by vibrational analyses; ZPE and thermal (enthalpy and entropy) corrections (1 bar, 273 K) from these analyses are included. All energies mentioned in the text are free energies.

Results and Discussion

The Basic Model: Cp₂ZrMe⁺. Let us for the moment use the methyl group as an (admittedly minimal) model of a polymer chain; the complications associated with larger alkyl groups will be discussed below. The complete path is summarized in Figure 1, and relative energies are collected in Table 1.

Ethene insertion in Cp₂ZrMe⁺ has been studied by several groups.¹⁵ The reaction follows a path similar to the Cossee–Arlmann mechanism¹⁶ with α -agostic assistance;¹⁷ the barrier between the π -complex **2** and the insertion transition state **3** is small or possibly non-existent. With the basis set and functional used here,

(11) De Angelis, F.; Sgamellotti, A.; Re, N. *Organometallics* **2000**, *19*, 4904.

(12) (a) Ahlrichs, R.; Bär, M.; Baron, H.-P.; Bauernschmitt, R.; Böcker, S.; Ehrig, M.; Eichkorn, K.; Elliott, S.; Furche, F.; Haase, F.; Häser, M.; Hättig, C.; Horn, H.; Huber, C.; Huniar, U.; Kattannek, M.; Köhn, A.; Kölmel, C.; Kollwitz, M.; May, K.; Ochsenfeld, C.; Öhm, H.; Schäfer, A.; Schneider, U.; Treutler, O.; Tsereteli, K.; Unterreiner, B.; Von Arnim, M.; Weigend, F.; Weis, P.; Weiss, H. Turbomole Version 5, January 2002; Theoretical Chemistry Group, University of Karlsruhe, Karlsruhe, Germany, 2002. (b) Treutler, O.; Ahlrichs, R. *J. Chem. Phys.* **1995**, *102*, 346.

(13) (a) PQS version 2.4; Parallel Quantum Solutions, Fayetteville, AR, 2001 (the Baker optimizer is available separately from PQS upon request). (b) Baker, J. *J. Comput. Chem.* **1986**, *7*, 385.

(14) (a) Lee, C.; Yang, W.; Parr, R. G. *Phys. Rev. B* **1988**, *37*, 785. (b) Becke, A. D. *J. Chem. Phys.* **1993**, *98*, 1372. (c) Becke, A. D. *J. Chem. Phys.* **1993**, *98*, 5648. (d) All calculations were performed using the Turbomole functional “b3-lyp”, which is not identical with the Gaussian “B3LYP” functional.

Table 1. Free Energies (in kcal/mol, Relative to the Metal Alkyls) for Species on the CO/Olefin Copolymerization Path

species	Cp ₂ ZrMe	Me ₂ SiCp ₂ ZrMe	Me ₂ SiInd ₂ ZrMe
1	0.0	0.0	0.0
2	-6.7	-7.5	-3.7
3	2.6	2.9	5.9
4	-13.4	-12.3	-9.7
5	4.0	7.4	6.1
6	-26.1	-24.4	-22.2
7a	-33.9	-33.8	-28.6
7b	-34.3		
8a	-21.0	-22.7	-15.9
8b	-24.9		
9	-12.2	-12.8	-8.3
10	-47.5	-47.0	-43.8
11a	-47.0	-47.5	-40.4
11b	-44.2		
12	-36.1	-36.5	-31.0
13	-50.1	-49.0	-42.9
14	-51.0	-50.7	-44.6
15	-37.3	-39.0	-31.9

we obtain a complexation free energy of 7 kcal/mol and a barrier of 4 kcal/mol. Addition of CO changes the chemistry significantly (Figure 2). CO is a stronger donor than ethene (complexation energy: CO, 13 kcal/mol; ethene, 7 kcal/mol); therefore, the most stable complex in the system will be Cp₂Zr(Me)(CO)⁺ (**4**). The barrier to CO insertion, however, is quite high: 17 kcal/mol. Alternatively, the system could displace CO by ethene, insert via transition state **3**, which is now 11 kcal/mol above the CO complex, and then regenerate the CO complex. Assuming the displacement of CO by ethene can follow an associative path and will not be rate limiting, the effective barrier for propagation has increased by 7 kcal/mol due to the presence of CO. The similarity of the two effective barriers suggests that (slow) propagation in the presence of CO, before its insertion, remains possible.

Insertion of CO follows the standard migratory insertion path. However, the *energy profile* of the reaction is somewhat unusual. Starting from complex **4**, the energy increases monotonically up till a point (**5**) one would normally classify as a σ -bound acyl. Then the acyl starts to turn its oxygen toward the Zr atom, to form an η^2 -acyl, and it is only at that point that the energy starts to decrease again. In other words, η^1 -acyl **5** is a transition state, *not* a local minimum as found for CO insertion in the neutral complex Cp₂ZrMe₂.¹¹ One important consequence is that the Zr–alkyl bond is already completely broken at the transition state. Therefore, anything that affects the strength of this bond affects the height of the insertion barrier directly. In view of the high insertion barrier and strong exothermicity of the CO insertion (13 kcal/mol counting from **4**), this step can be considered to be irreversible.

The final product of CO insertion is the η^2 -acyl species **6**. This could again coordinate and insert both CO and

(15) (a) Woo, T. K.; Fan, L.; Ziegler, T. *Organometallics* **1994**, *13*, 432, 2252. (b) Fusco, R.; Longo, L.; Masi, F.; Garbassi, F. *Macromolecules* **1997**, *30*, 7673. (c) Thorshaug, K.; Støvneng, J. A.; Rytter, E.; Ystenes, M. *Macromolecules* **1998**, *31*, 7149. (d) Meier, R. J.; Van Doremale, G. H. J.; Iarlori, S.; Buda, F. *J. Am. Chem. Soc.* **1994**, *116*, 7274. (e) Froese, R. D. J.; Musae, D. G.; Morokuma, K. *J. Mol. Struct. (THEOCHEM)* **1999**, *461–462*, 121.

(16) (a) Cossee, P. *J. Catal.* **1964**, *3*, 80. (b) Arlman, E. G.; Cossee, P. *J. Catal.* **1964**, *3*, 99.

(17) (a) Grubbs, R. H.; Coates, G. W. *Acc. Chem. Res.* **1996**, *29*, 85. (b) Brintzinger, H. H.; Fischer, D.; Mühlaupt, R.; Rieger, B.; Waymouth, R. M. *Angew. Chem., Int. Ed. Engl.* **1995**, *34*, 1143.

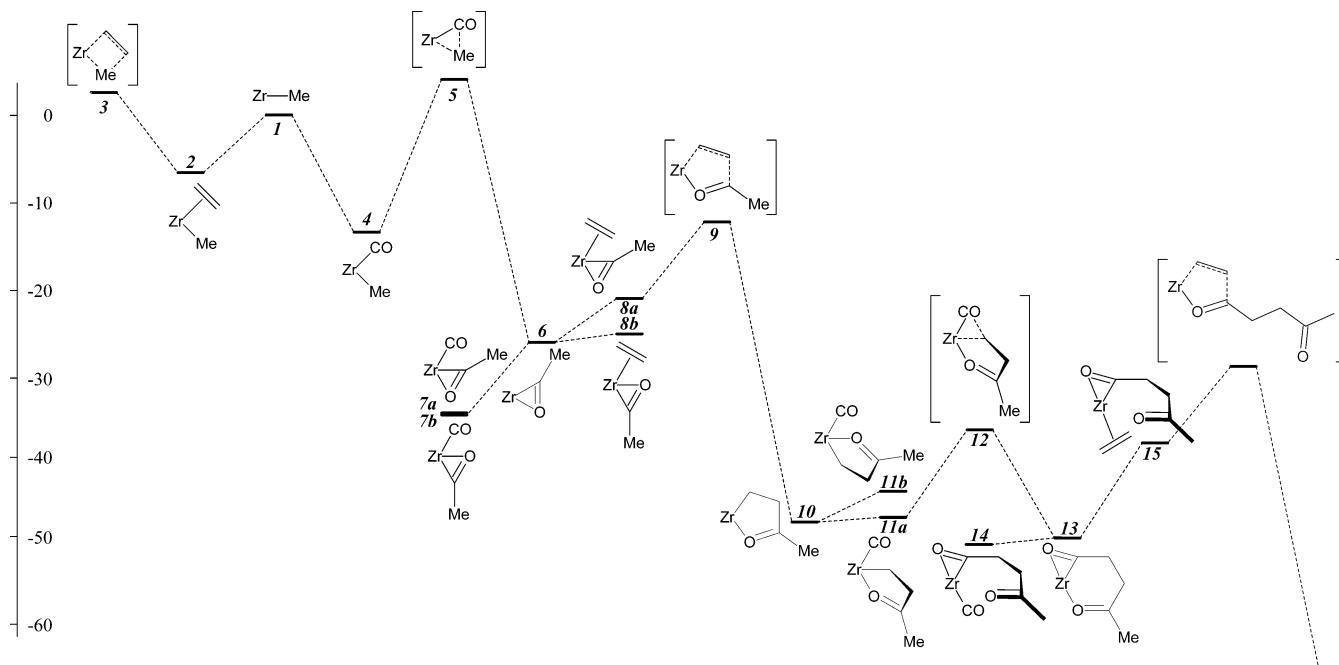


Figure 1. Reaction path for CO/ethene copolymerization starting with Cp_2ZrMe^+ . Relative free energies are given in kcal/mol.

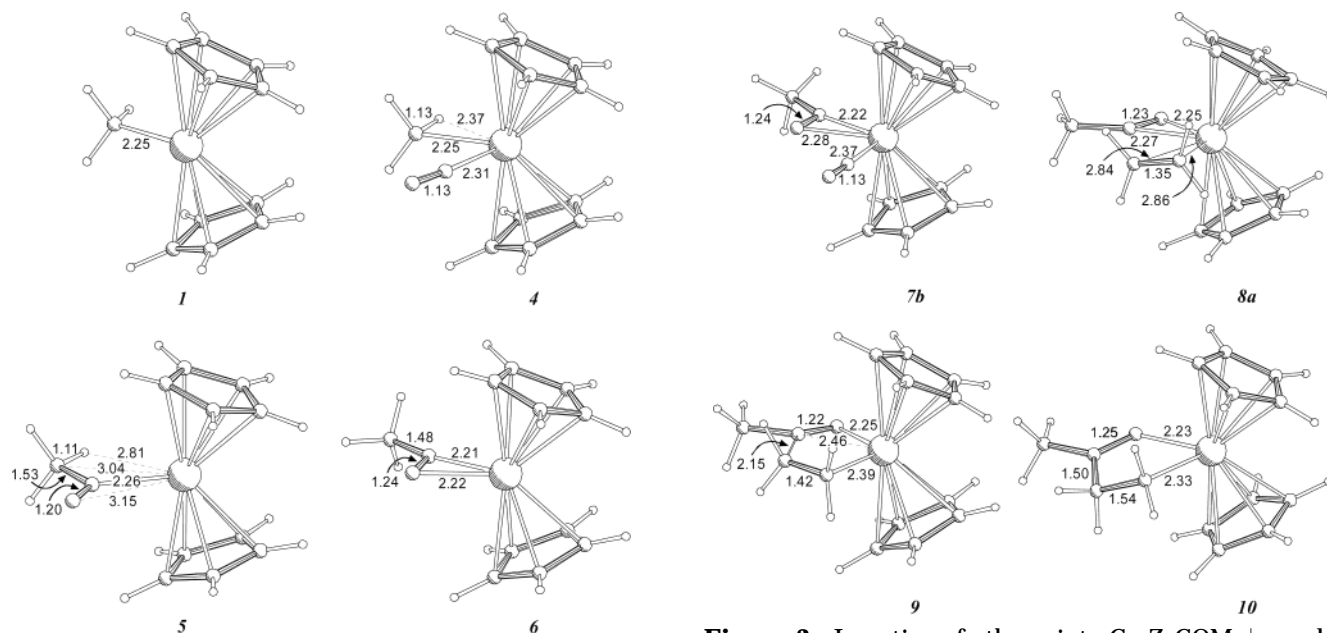


Figure 2. Insertion of CO into Cp_2ZrMe^+ : alkyl (**1**), CO complex (**4**), transition state (**5**), and η^2 -acyl product (**6**).

ethene. CO coordination produces either **7a** ("O out") or **7b** ("O in"); the calculated energy difference of 0.4 kcal/mol in favor of **7b** agrees nicely with the observed equilibrium ratio of 5:1 observed experimentally (Figure 3).⁹ Double CO insertion is presumably thermodynamically unfavorable and was not considered here. However, CO coordinates much more strongly than ethene to the acyl; thus, for subsequent insertions $\text{Cp}_2\text{Zr}(\eta^2\text{-MeCO})(\text{CO})^+$ (**7b**) is the resting state and reference point. Displacing CO by ethene (to give **8a**) costs 13 kcal/mol. From the olefin complex on, the insertion barrier is only 9 kcal/mol, so that the effective barrier is ca. 22 kcal/mol. The transition state **9** has a fully broken Zr–

Figure 3. Insertion of ethene into $\text{Cp}_2\text{ZrCOME}^+$: acyl–CO complex resting state (**7b**), acyl–ethene complex (**8a**), insertion transition state (**9**), and insertion product (**10**).

C_{acyl} bond and a strong Zr–O interaction. Clearly, coordination of the oxygen to Zr assists the insertion.¹⁸

After the insertion, we obtain five-membered-ring chelate structure **10**. This is extremely stable, as is evident from the exothermicity of its formation (21 kcal/mol from the η^2 -acyl, which is itself already stabilized by a Zr–O interaction). Thus, we expected that neither ethene nor CO would be able to displace the carbonyl oxygen from Zr. However, we find that CO can coordinate *without* displacing the oxygen, producing the

(18) We have also considered a path where the acyl first rotates to an $\eta^1(\text{C})$ -bound structure. This does give a true transition state leading to the correct product, but the barrier is so much higher than for the path maintaining the Zr–O interaction that we have not considered it further.

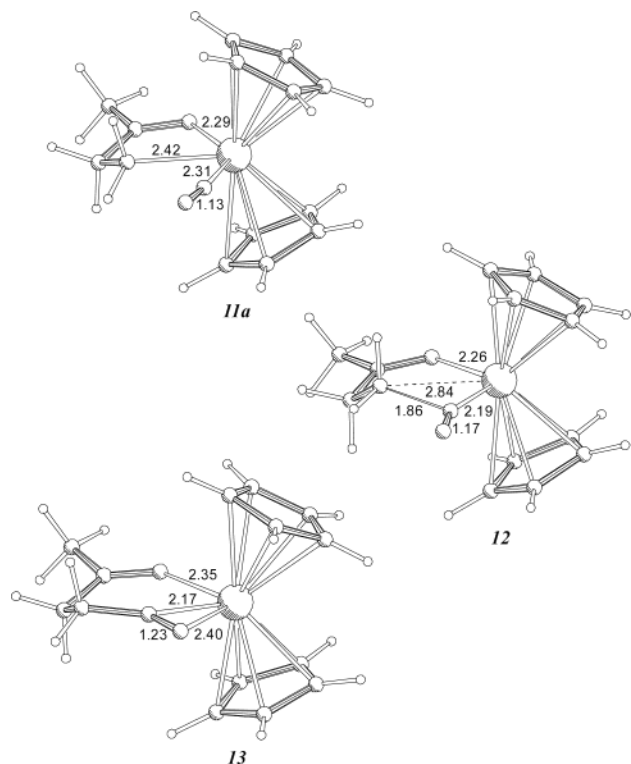


Figure 4. CO insertion into the $\text{Cp}_2\text{ZrCH}_2\text{CH}_2\text{COMe}^+$ chelate: CO complex (**11a**), insertion transition state (**12**), and insertion product (**13**).

formally 18e species **11** (Figure 4). This complexation is slightly uphill (1 kcal/mol) for entropic reasons. Insertion of the CO molecule in the Zr–C bond then is rather easy, requiring only 10 kcal/mol (cf. 17 kcal/mol for formation of **4**). Ethene, which is much bulkier than CO, does not coordinate as strongly and hence does not insert as easily. In other words, carbonyl coordination in the chelate blocks ethene insertion but actually assists CO insertion!

Once the second CO is inserted, we are left with η^2 -acyl species **13** bearing an internally coordinating carbonyl group. This $5^{1/2}$ -membered chelate ring is somewhat strained, and as a consequence opening of the ring by CO or ethene to give **14** or **15** is not difficult (Figure 5). CO will not insert, but ethene will. Since there is no direct Zr–carbonyl interaction in the ring-opened ethene complex **15**, the barrier for ethene insertion from **15** should be similar to that for **8a**, and the effective barrier, counting from CO complex **14**, should be similar to the energy difference between **7a** and **9**. In other words, the second ethene insertion should have the same effective barrier as the first (ca. 22 kcal/mol).

Influence of the Alkyl Group at Zr. CO quenching is used to “count” primary and secondary alkyl chains at the metal. Therefore, the relative efficiency of trapping either kind of chain with CO is important. If secondary chains would be trapped rapidly but primary chains could grow on for a long time, counting could produce a skewed picture of their relative amounts.

We see three different effects on going from a simple methyl group to the larger ethyl and isopropyl groups (Table 2). First, longer chain alkyls **1** always have a β -agostic Zr–H interaction. This is lost on ethene and CO coordination. Thus, the complexation energies of CO

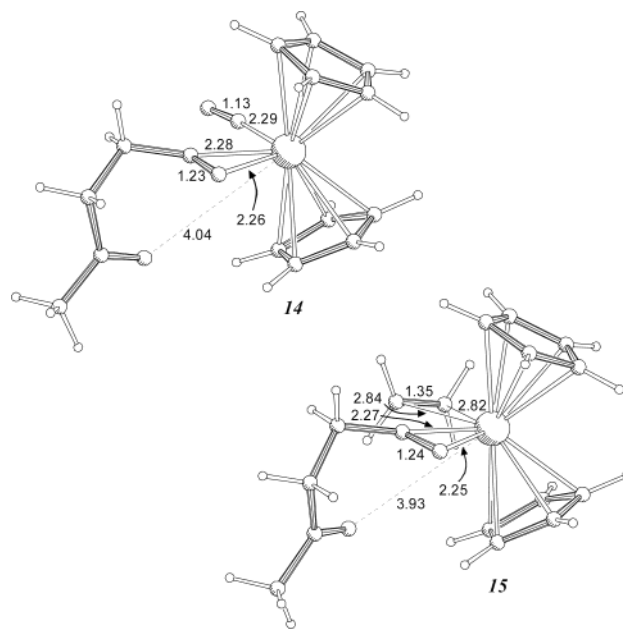


Figure 5. Opening of $\text{Cp}_2\text{ZrCOCH}_2\text{CH}_2\text{COMe}^+$ by CO (**14**) and ethene (**15**).

Table 2. Free Energies (in kcal/mol, Relative to the CO Complexes) for Initial Ethene and CO Insertion Steps

species	Cp_2Zr			$\text{Me}_2\text{SiCp}_2\text{Zr}$		$\text{Me}_2\text{SiInd}_2\text{Zr}$	
	Me	Et	<i>i</i> Pr	Me	Et	Me	Et
1	13.4	5.2	5.4	12.3	6.8	9.7	3.2
2	6.7	10.1	11.5	4.8	9.1	6.0	6.9
3	16.0	15.1	15.5	15.2	14.6	15.6	13.5
4	0.0	0.0	0.0	0.0	0.0	0.0	0.0
5	17.4	14.6	11.8	19.7	17.6	15.8	11.9
6	-12.7	-15.3	-18.2	-12.1	-14.1	-12.5	-16.5

and ethene decrease because of the somewhat artificial change in reference point. This is the reason the energies in Table 2 are given relative to the CO complexes instead of the naked alkyls. However, this in itself would not affect the relative barriers for CO and ethene insertion. The second effect is steric. The size difference among Me, Et, and *i*Pr has a significant effect on the ethene complexation energy, but because of the much smaller size of CO it does not affect the CO complexation energy much. Insertion transition states are less sensitive to this steric effect, so again the effect on insertion barriers is small. Finally, the Zr–alkyl bond is destabilized by increased substitution at the α -carbon. Since this bond is completely broken at the CO insertion TS, but not at the olefin insertion TS, there is a clear effect on the balance between CO and ethene insertion. Each α -substituent decreases the barrier for CO insertion by ca. 3 kcal/mol, while (relative to the CO complex) the olefin insertion barrier does not change much. Thus, secondary alkyls are more efficiently trapped by CO than primary alkyls.

Ligand Effects: Cp_2Zr , $\text{Me}_2\text{SiCp}_2\text{Zr}$, and $\text{Me}_2\text{SiInd}_2\text{Zr}$. CO coordination to $\text{Me}_2\text{SiCp}_2\text{ZrMe}^+$ is slightly weaker than to Cp_2ZrMe^+ (ca. 1 kcal/mol). In contrast, ethene coordinates more strongly to the same system (ca. 1 kcal/mol), which agrees with the higher sensitivity of ethene coordination to steric effects. The ethene insertion barrier is comparable to that for Cp_2ZrMe^+ , but the CO insertion barrier is clearly higher (by ca. 3

kcal/mol, counting from the CO complex). The CO insertion transition state is basically a Zr acyl lacking any stabilizing interactions; it is reasonable that this would be less favorable in combination with the more open, less saturated $\text{Me}_2\text{SiCp}_2\text{Zr}$ fragment. The net effect of these changes is that CO insertion becomes about 3 kcal/mol more difficult *relative* to ethene insertion.

Going on to the $\text{Me}_2\text{SiInd}_2\text{Zr}$ system, we find decreased CO and ethene coordination energies (by ca. 3 kcal/mol). CO insertion now becomes *easier* relative to ethene insertion, by about 3 kcal/mol relative to Cp_2Zr . In this respect, the $\text{Me}_2\text{SiInd}_2\text{Zr}$ system behaves as less unsaturated than $\text{Me}_2\text{SiCp}_2\text{Zr}$ or even Cp_2Zr . This is also reflected in subsequent CO coordination energies. In the order Cp_2Zr , $\text{Me}_2\text{SiCp}_2\text{Zr}$, and $\text{Me}_2\text{SiInd}_2\text{Zr}$ they are as follows: for **6** \rightarrow **7a**, -6.8 , -9.4 , -6.4 kcal/mol; for **10** \rightarrow **11a**, $+0.5$, -0.5 , $+3.4$ kcal/mol.

The subsequent ethene insertion step is hardly affected by the changes in ligand structure, but interestingly, the second CO insertion step shows a trend opposite to the first one: slightly easier for $\text{Me}_2\text{SiCp}_2\text{Zr}$ and slightly more difficult for $\text{Me}_2\text{SiInd}_2\text{Zr}$. On the whole, however, the only large (>2 kcal/mol) changes are seen in the first CO insertion barrier.

Expectations for CO Quenching of Polymerization. Both ligand structure and the alkyl chain have a significant effect on the balance between olefin insertion (propagation) and the first CO insertion. In addition, insertion of propene in the Zr-alkyl bond is more difficult than ethene insertion by ca. 4 kcal/mol.¹⁹ This should be taken into account when comparing propagation and CO insertion barriers.

For Cp_2Zr , CO and ethene insertion in a primary alkyl are closely matched. For $\text{Me}_2\text{SiCp}_2\text{Zr}$, ethene insertion is preferred in a primary chain; for a secondary chain, or for propene and a primary chain, the difference should be small. For $\text{Me}_2\text{SiInd}_2\text{Zr}$, CO insertion is easiest and should normally be preferred. However, the preference is not extreme and at low CO pressures competing olefin insertion cannot be excluded.

Once CO has inserted, subsequent olefin insertion has a significant barrier. In the presence of excess CO, the resting state will be the $\text{L}_2\text{Zr}(\text{CO})(\eta^2\text{-acyl})^+$ complex, and a barrier of about 20 kcal/mol can be expected. For low CO concentrations, the relevant resting state shifts toward $\text{L}_2\text{Zr}(\eta^2\text{-acyl})^+$, and the olefin insertion barrier will be reduced to 12–14 kcal/mol. The following *second* CO insertion has a barrier of 10–13 kcal/mol, which will become higher at low CO concentrations. The end result can be summarized as follows:

At high CO concentrations, CO will coordinate, which is sufficient to completely quench polymerization. The CO insertion rate depends on the system, but the insertion barrier is significant and one cannot assume all growing chains to incorporate CO if the quenched reaction is worked up at low temperature. After CO insertion, subsequent olefin insertion is possible but slow; each olefin that inserts will immediately be followed by a CO unit. Single-CO insertion has indeed been verified in the quenching of Cp_2Zr -catalyzed polymerization of propene with high pressures of CO.⁶ In

many cases, however, single-CO incorporation has simply been *assumed* to be quantitative and limited to one CO per chain. Our results suggest that this assumption may not always be valid.

At low CO concentrations, the propagation resting state immediately becomes $\text{L}_2\text{Zr}(\text{R})(\text{CO})^+$, slowing down propagation strongly. However, some olefin units may still insert before the relatively slow CO insertion occurs. After the first CO insertion, subsequent olefin and CO insertions will occur alternately. The barriers for these steps can be similar, depending on the CO concentration; both can be faster than the first CO insertion. Busico reported that the main end groups visible by NMR are *ketones*, derived from *primary* alkyls, and *aldehydes*, derived from *secondary* alkyls.⁷ This appears to be consistent with our observation that (a) olefin and CO insertion barriers are comparable and (b) CO insertion is easier in secondary alkyls. However, since we have not studied propene insertion at all, this explanation must remain tentative.

Comparison of Early (Zr) and Late (Pd) Transition Metals. The Pd-catalyzed alternating copolymerization of CO and ethene has been studied in detail, both experimentally²⁰ and theoretically.²¹ Inspection of the relevant energies shows that, perhaps surprisingly, there are more similarities than differences between the two types of systems. CO coordinates more strongly than ethene by about 6 kcal/mol in both systems, and even the calculated CO binding energies of Cp_2ZrEt^+ and $(\text{H}_2\text{-PCH=CHPH}_2)\text{PdEt}^+$ are similar.²² The CO and ethene insertion barriers observed ($\Delta G^\ddagger = 13.4$ and 12.3 kcal/mol for $(\text{dppp})\text{Pd}^{20a}$) and calculated ($\Delta H^\ddagger = 11.5$ and 13.9 kcal/mol for $(\text{H}_2\text{PCH=CHPH}_2)\text{Pd}^{21a}$) for the Pd system are fairly similar to those calculated here for **10** \rightarrow **12** and **6** \rightarrow **9** ($\Delta G^\ddagger = 11$ and 13 kcal/mol). The main difference is in the *first* CO insertion step (**4** \rightarrow **5**), which for Zr can have a higher barrier (12–18 kcal/mol, depending on the ligand) than later CO insertions.

Another important difference with Pd is that, in the *absence* of CO, zirconocenes are much more active in olefin homopolymerization. The calculated homopolymerization barrier for Zr, counting from the olefin complex (**2** \rightarrow **3**, ethene in Zr-Et) is ca. 5 kcal/mol, which should be contrasted with an experimental ΔG^\ddagger of 16.3 kcal/mol for $(\text{dppp})\text{Pd}^{20a}$ and a calculated ΔH^\ddagger of 15.5 kcal/mol for $(\text{H}_2\text{PCH=CHPH}_2)\text{Pd}$.^{21a} Thus, the slowdown of reactivity by CO addition is much more dramatic for Zr than for Pd.

If we look at *geometries* of intermediates and transition states, further differences emerge. Olefin insertion into the Pd-acyl bond involves initial conversion of the η^2 -acyl group to a perpendicular $\eta^1(\text{C})$ orientation, in which the metal-oxygen interaction has been lost (Scheme 3). In contrast, the much more oxophilic Zr

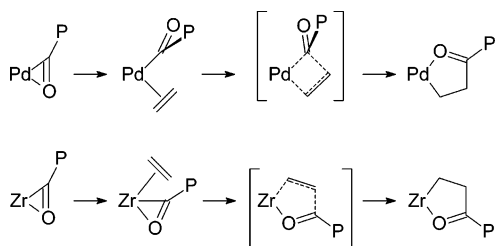
(20) (a) Shultz, C. S.; Ledford, J.; DeSimone, J. M.; Brookhart, M. *J. Am. Chem. Soc.* **2000**, *122*, 6351. (b) Ledford, J.; Shultz, C. S.; Gates, D. P.; White, P. S.; DeSimone, J. M.; Brookhart, M. *Organometallics* **2001**, *20*, 5266. (c) Rix, F. C.; Brookhart, M.; White, P. S. *J. Am. Chem. Soc.* **1996**, *118*, 4746.

(21) (a) Margl, P.; Ziegler, T. *J. Am. Chem. Soc.* **1996**, *118*, 7337. (b) Svensson, M.; Matsubara, T.; Morokuma, K. *Organometallics* **1996**, *15*, 5568. (c) Frankcombe, K. E.; Cavell, K. J.; Yates, B. F. *Organometallics* **1997**, *16*, 3199.

(22) Margl and Ziegler^{21a} did not calculate free energies. Excluding ZPE and thermal corrections, the calculated CO binding energies are 16.7 kcal/mol for Cp_2ZrEt^+ (this work) and 18.6 kcal/mol for $(\text{HPCH=CHPH})\text{PdEt}^+$.^{21a}

(19) Borrelli, M.; Busico, V.; Cipullo, R.; Ronca, S.; Budzelaar, P. H. M. *Macromolecules* **2002**, *35*, 2835.

Scheme 3



center retains contact with oxygen but has lost interaction with the acyl carbon in the planar five-center transition state **9**. In the subsequent CO insertion step, the Pd system opens the $\text{MCH}_2\text{CH}_2\text{COR}$ chelate ring to accommodate the incoming CO ligand. This is not possible with Zr. Instead, we find an associative mechanism in which carbonyl coordination is retained over the whole sequence **10** \rightarrow **11** \rightarrow **12** \rightarrow **13**. Thus, the consequences of oxophilicity and strong coordinative unsaturation of the Zr center are expressed more clearly in the *geometries* than in the *energies* of the species on the copolymerization path.

Conclusions

CO/olefin copolymerization at zirconocenes is by no means a fast and easy reaction. In view of the high oxophilicity of Zr, the fact that it proceeds at all is already remarkable. Our calculations suggest that two factors are important here. In the first place, the stable chelate **10** can coordinate and then insert a CO molecule *without* losing the Zr–carbonyl coordination. This is crucial, since *displacement* of the carbonyl by CO would probably be prohibitively expensive. Second, carbonyl coordination appears to be weaker in the $5^{1/2}$ -membered carbonyl–acyl species **13**, and here even ethene can displace the carbonyl and then insert. The availability to zirconocene–alkyl cations of *two* additional coordina-

tion sites is essential, and it might well be that octahedral systems having only a single empty site available for chain growth (like the presumed active species in heterogeneous Ziegler–Natta catalysis) would be completely blocked by CO at the chelate stage.

Even for zirconocenes, CO has an inhibiting effect on olefin insertion, and our results suggest it can be safely used for chain counting, *provided* it is used in a large excess, and temperature and reaction time are chosen such that CO insertion does occur but subsequent olefin insertion is still suppressed. These conditions are not the ones typically used for chain counting. In particular, the use of small quantities of (radioactive) ^{14}C O is generally preferred. We propose using instead a large excess of *diluted* ^{14}C O (in ^{12}C O) to ensure efficient quenching of polymerization.

As for preparing oligoketone-functionalized polyolefins, the main problem is probably chain transfer and reinitiation after CO “termination”. The functionalized polymers are reactive enough to bind aluminum alkyls and MAO commonly used as scavengers; thus, the polymerization would require several equivalents of scavenger per chain. Also, the process would have to be divided into separate olefin and CO/olefin growth steps, since just adding small amounts of CO during polymerization would cause an unacceptable slowdown of polyolefin growth. The resulting process might well become too complex to be practical.

Acknowledgment. I thank Prof. Vincenzo Busico for valuable discussions and am grateful to Sabic EPC for financial assistance.

Supporting Information Available: A table giving total energies and thermal corrections for all molecules studied. This material is available free of charge via the Internet at <http://pubs.acs.org>. Optimized geometrical parameters for all species are available on request from the author.

OM0342863